

SCIENTIFIC REPORTS



OPEN

Ratiometric fluorescent probe with AIE property for monitoring endogenous hydrogen peroxide in macrophages and cancer cells

Yong Liu¹, Jing Nie², Jie Niu¹, Fangfang Meng¹ & Weiyong Lin¹

Hydrogen peroxide (H_2O_2) plays a key role in the progression of human illnesses, such as autoimmune and auto-inflammatory diseases, infectious diseases, diabetes, and cancer, etc. In this work, we have described a novel probe, TPE-TLE, which remarkably displayed AIE property and ratiometric fluorescence emission profiles in the presence of H_2O_2 . This ratiometric fluorescent probe with AIE property exhibits outstanding features such as the well-resolved emission peaks, high sensitivity, high selectivity, low cytotoxicity, and good cell-membrane permeability. These excellent attributes enable us to demonstrate the ratiometric imaging of endogenously produced H_2O_2 in macrophages and cancer cells based on the novel ratiometric probe with AIE property for the first time. By comparing two kinds of cells, it is firstly found that cancer cells should contain much more endogenous H_2O_2 than macrophages. We expect that TPE-TLE will be useful fluorescent platform for the development of a variety of ratiometric fluorescent probes with AIE property to achieve unique biological applications.

In 2001, the novel phenomenon of aggregation-induced emission (AIE) was first found by Tang's group¹. AIE materials show very weakly fluorescence features in solution state and became intense in the aggregated state^{2,3}. The above unique finding has become a new method to tackle the aggregation-caused quenching (ACQ) of conventional chromophores and has shown significant academic value and promising applications in cell imaging⁴, fluorescent sensors and bio-probe materials^{5,6}. Herein, we describe the development of a novel ratiometric fluorescent probe with AIE property for ratiometric monitoring bioactive small molecule in the living system.

Reactive oxygen species (ROS) are formed as a natural by-product of the normal metabolism of oxygen and play a key role in cell signaling and homeostasis⁷⁻⁹. Generation of excessive ROS is involved in the pathogenesis of various diseases such as cardiovascular disease, cancer and neurological disorders¹⁰⁻¹². Hydrogen peroxide (H_2O_2), a major ROS, exhibits relatively mild reactivity and has attracted intense interest¹³⁻¹⁷. Because it appears to be involved in signal transduction by reversible oxidation of proteins¹⁸. It has been known for many years that H_2O_2 plays a major role in the progression of human illnesses, such as autoimmune and auto-inflammatory diseases, infectious diseases, diabetes, mutagenesis and, perhaps most importantly, cancer¹⁹⁻²³. Consequently, the search for a method that can be used for monitoring H_2O_2 has always been attractive and challenging.

Owing to the transient nature of H_2O_2 , fluorescent probes, which generally display high sensitivity and can be used to determine spatial and temporal distributions in live specimens, are particularly appealing tools for the detection of ROS and related metabolites²⁴. Most of these probes are intensity-based type, and tend to be interfered by the variations in excitation intensity, probe concentration, etc. To alleviate these problems, a number of ratiometric fluorescent H_2O_2 probes have been developed^{25,26}. However, up to present, there have been no reports on an AIE material for ratiometric sensing and imaging endogenous H_2O_2 in living cells (Table S1). Thus, developing ratiometric fluorescent probe with AIE property is very important due to significant academic value and biological applications of AIE materials. Thus, the goal of our work is to design a ratiometric fluorescent probe with AIE property for ratiometric detecting H_2O_2 in different cell lines.

¹Institute of Fluorescent Probes for Biological Imaging, School of Chemistry and Chemical Engineering, School of Materials Science and Engineering, University of Jinan, Jinan, Shandong, 250022, P.R. China. ²School of Chemical Engineering & Technology, China University of Mining and Technology, Xuzhou, Jiangsu, 221116, P.R. China. Yong Liu and Jing Nie contributed equally to this work. Correspondence and requests for materials should be addressed to W.L. (email: weiyonglin2013@163.com)

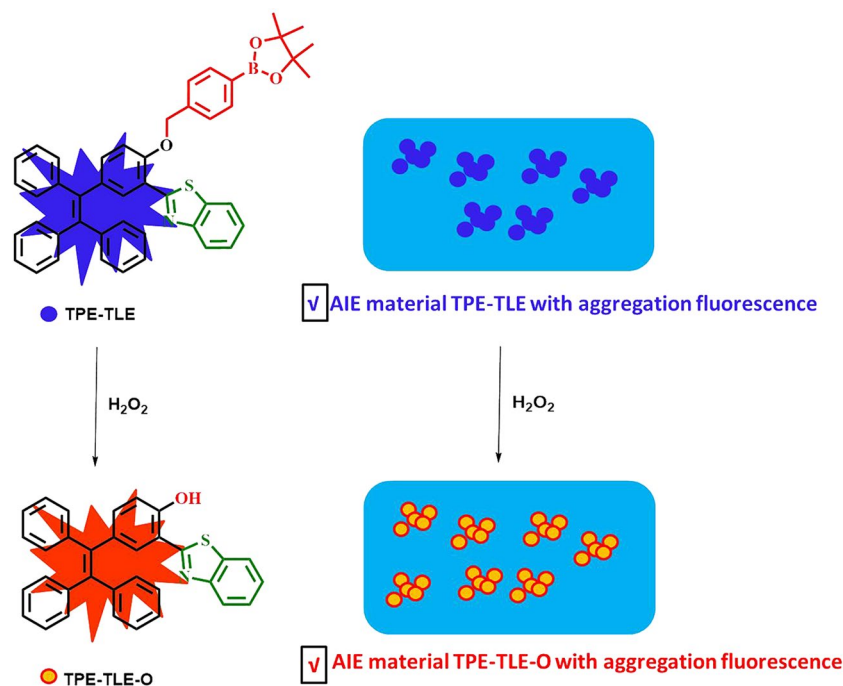


Figure 1. The sense mechanism of the probe TPE-TLE to H₂O₂.

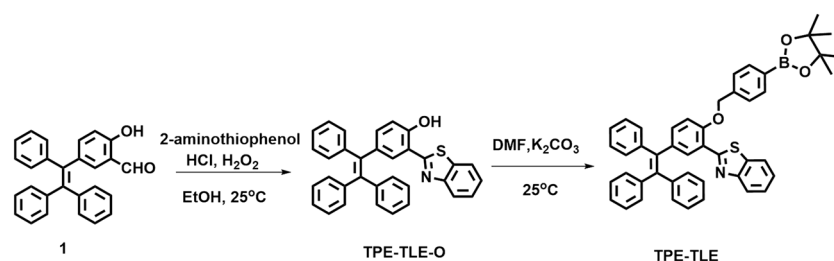


Figure 2. The synthetic routes of the compound TPE-TLE.

In this work, we described a novel ratiometric H₂O₂ fluorescent probe with AIE property for the first time. This ratiometric fluorescent probe with AIE property exhibits outstanding features such as the well-resolved emission peaks, high sensitivity, high selectivity, low cytotoxicity, and good cell-membrane permeability. These features were promising this novel AIE material can be successfully applied for ratiometric imaging endogenous H₂O₂ in living RAW 264.7 macrophages and cancer cells HepG2. Compared to RAW 264.7 macrophages, we firstly found that cancer cells HepG2 should contain much more endogenous H₂O₂.

Results and Discussion

Preparation of probe. As we all know, tetraphenylethene (TPE) is an archetypal AIE luminogen²⁷. On the basis of our interest on AIE material²⁸, we further exploited the unique application of this class of dyes by rational structural modifications. As shown in Fig. 1, we introduced a thiazole group on the TPE-core to afford the novel AIE material TPE-TLE-O. On the other hand, modification of a H₂O₂ site such as a borate moiety on the TPE-TLE-O gave the new compound TPE-TLE, which exhibited AIE character distinguishing from TPE-TLE-O. We envision that both materials exhibit distinct aggregation fluorescence signals.

For the AIE material TPE-TLE, in the presence of H₂O₂, the oxidation reaction of H₂O₂ to the borate moiety will provide TPE-TLE-O, which will decrease aggregation fluorescence signal of TPE-TLE to induce aggregation fluorescence signal of TPE-TLE-O. Therefore, we envisioned that AIE material TPE-TLE may be suitable for ratiometric imaging endogenous H₂O₂ in living systems.

Chemical synthesis of the compound TPE-TLE was accomplished in a total of two steps (Fig. 2). The compound TPE-TLE-O was prepared by the ring-closing reaction between compound 1 and 2-aminothiophenol. TPE-TLE was synthesized by a substitution reaction. The ¹H NMR, ¹³C NMR, and H RMS were given in the Supporting Information.

Optical properties in various solvents. Optical properties of probes were basic properties of compounds. These properties provided clues for speculating its optical applications. Thus, with TPE-TLE in hand, we first

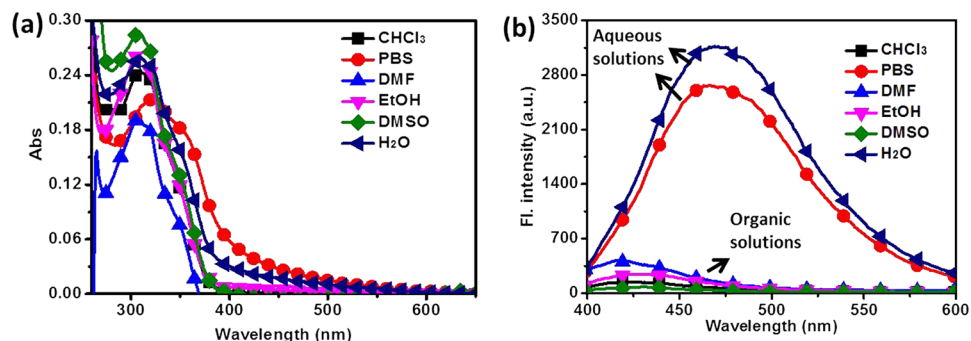


Figure 3. (a) The UV-vis absorption and (b) fluorescence spectra of TPE-TLE in aqueous solutions and organic solvents. [TPE-TLE] = 5.0 μ M.

evaluated its absorption and fluorescence profile in aqueous solutions and organic solutions. As shown in Fig. 3 and Table S2, our studies revealed that TPE-TLE had absorption and emission peak at 305 nm and 475 nm in aqueous solutions; In organic solutions, the absorption and emission peak of probe emerged at 305 nm and 420 nm. The results indicated that this probe had larger Stokes shift in aqueous solutions than organic solvents. Moreover, the probe exhibited higher fluorescence quantum yield ($\Phi = 0.61$) in pure water system than organic solvents ($\Phi = 0.02$ in EtOH). As anticipated, the aggregation of the compound TPE-TLE may affect optical physical properties of compound in pure water system. Introduction of a thiazole group on the TPE-core will obtain a novel AIE material TPE-TLE.

AIE property. To verify the compound TPE-TLE whether was a fluorescent material with AIE property, we investigated optical properties of TPE-TLE in the distinct polar environments. We set out to investigate the fluorescence behavior of TPE-TLE in water/DMF (f_w) mixtures. Firstly, we prepared eleven organic solutions of TPE-TLE with different water fraction (f_w); Photographs of TPE-TLE in water/DMF mixtures were taken under UV illumination (Fig. 4a). The above result demonstrated that the blue fluorescence signal of TPE-TLE gradually became strong when f_w increased from 0% ($\Phi = 0.11$) to 100% ($\Phi = 0.61$). Secondly, we systematically changed f_w value, and further measured the emission spectra of TPE-TLE in water/DMF mixtures (Fig. 4b). Fluorescence trend present gradually strong with increasing of f_w values (Fig. 4c). Fluorescence characteristics of TPE-TLE were consistent with photographs of TPE-TLE in the distinct polar environments. Thus, we predicted that the compound TPE-TLE should be a fluorescent material with AIE property. The optical studies of TPE-TLE revealed that rational structural modifications on the TPE-core could exhibit AIE character.

In preparation of probe, we have envisioned that the oxidation reaction of H_2O_2 to the borate moiety will provide TPE-TLE-O in the presence of H_2O_2 , which will decrease aggregation fluorescence signal of TPE-TLE to induce aggregation fluorescence signal of TPE-TLE-O. The TPE-TLE-O should be an AIE material distinguishing from TPE-TLE. To prove the above assumption, we investigated optical properties of TPE-TLE-O in the distinct polar environments. As shown in Fig. 5, photographs and fluorescence characteristics of TPE-TLE-O in water/DMF mixtures indicated that the compound TPE-TLE-O was an AIE material distinguishing from TPE-TLE.

The AIE material TPE-TLE should be suitable for ratiometric detecting H_2O_2 based on an aggregation emission method.

Ratiometric responses of probe TPE-TLE to H_2O_2 . To examine whether probe TPE-TLE could ratiometric detect H_2O_2 , TPE-TLE (5 μ M) was treated with H_2O_2 in PBS buffer solution (containing 50% DMF), and further studying the progress of the reaction by fluorescence titration experiment. As shown in Fig. 6a, in the absence of H_2O_2 , the probe TPE-TLE exhibited no visible variations in the ratios of emission intensities at 435 nm, suggesting that TPE-TLE was stable in the assay conditions. When increasing concentrations of H_2O_2 were introduced, the fluorescence spectra of probe TPE-TLE exhibited significant changes. The intensity of the emission maximum at 435 nm was gradually decreased with the simultaneous appearance of a new red-shifted emission band centered at 550 nm. The red-shift in the excitation spectra of the TPE with the increase H_2O_2 is due to intramolecular charge-transfer (ICT)^{29,30}. Moreover, the ratios of emission intensities at 550 and 435 nm (I_{550}/I_{435}) displayed a large increase from 0 to 4.25 (Fig. 6a, inset). Furthermore, a new fluorescence emission peak was observed at 550 nm. This result suggests that a new compound was formed during the titration process. The reaction product TPE-TLE-O was confirmed using 1H NMR (Fig. S1). The AIE material TPE-TLE was capable of detecting H_2O_2 by an aggregation emission method.

Sensitivity was an important criterion for developing highly sensitive fluorescence imaging agents³¹. Mainly reason was that the pathophysiologic ally relevant concentrations of H_2O_2 were in the low to medium micro molar concentrations³². We further investigate sensitive of probe in order to prove whether TPE-TLE can detect H_2O_2 in intercellular environment. As shown in Fig. 6b, the detection limit of the probe was 6.0 μ M, indicating that the probe TPE-TLE exhibited highly sensitive to H_2O_2 by an aggregation emission method. We expect that the probe TPE-TLE was able to detect low micro molar concentrations of H_2O_2 and possessed potentially applicable in medical and biological.

To demonstrate the selectivity of TPE-TLE to H_2O_2 , TPE-TLE was treated with a wide variety of cations, anions, and oxidants, and then fluorescence spectra were further measured. As shown in Fig. 6c and d, the probe

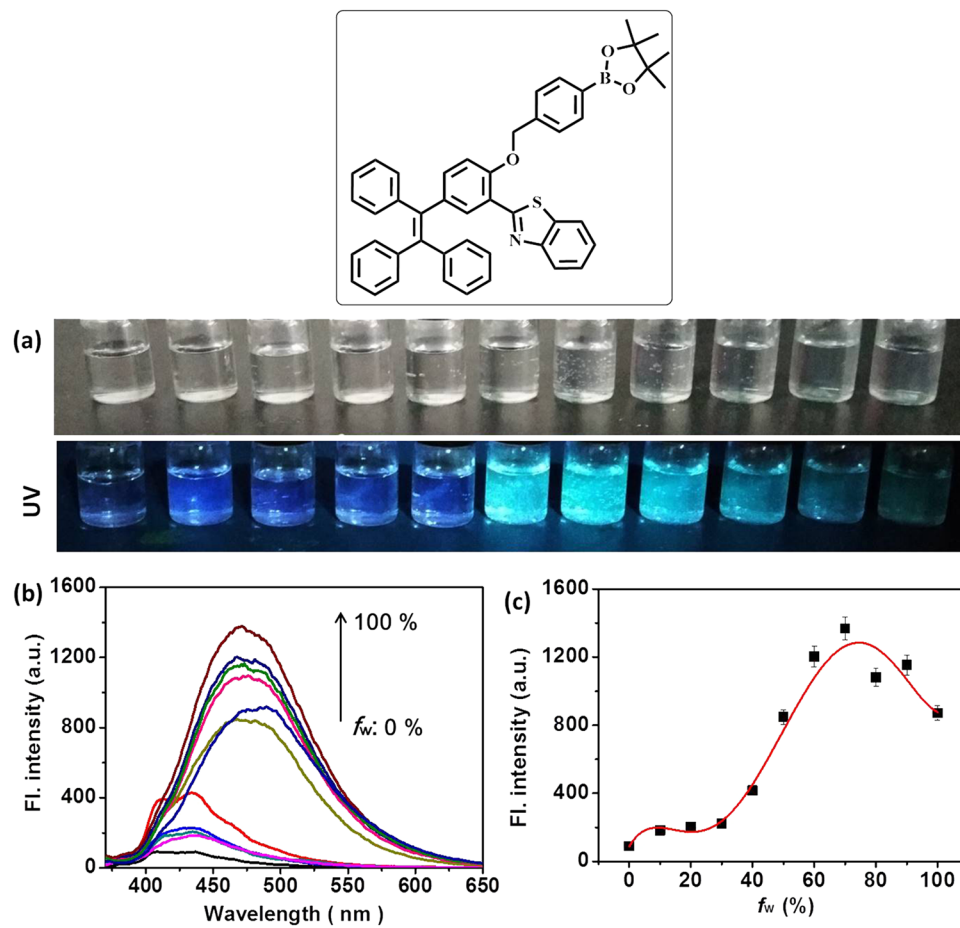


Figure 4. (a) Photographs of TPE-TLE in water/DMF mixtures taken under nature light and UV illumination; (b) Fluorescence spectra of TPE-TLE in water/DMF mixture; (c) Plots of maximum emission intensity of TPE-TLE in water/DMF mixtures with different f_w values. [TPE-TLE] = 5.0 μ M. λ_{ex} = 365 nm. The error bars represent standard deviation (\pm S.D.).

TPE-TLE exhibited a significant red-shift of the fluorescence emission spectra in the presence of H_2O_2 . Other representative species such as Ca^{2+} , Na^+ , K^+ , ClO^- , NO_2^- , NO_3^- , OH^- , 1O_2 , H_2O_2 , NO, TBHP, Cys, and GSH were added to TPE-TLE solutions. H_2O_2 elicited a large ratiometric signal with I_{550}/I_{435} . By contrast, other species induced a very low ratiometric response with I_{550}/I_{435} . This clearly indicated that the probe TPE-TLE had an excellent selectivity to H_2O_2 over the other analytes. The AIE material TPE-TLE was capable of highly selective detecting H_2O_2 by an aggregation emission method. In addition, the time-dependent fluorescence intensity changes from the probe TPE-TLE to H_2O_2 were further studied. As shown in Fig. S2, the probe TPE-TLE to H_2O_2 revealed that the reaction can be completed about 3 h.

We conducted another experiment condition to show that the probe can detect H_2O_2 in a ratiometric fashion *in vitro*. To examine the ratiometric fluorescence response of probe TPE-TLE to H_2O_2 , the probe was titrated with different equiv. of H_2O_2 in 90% PBS buffer solution (containing 10% DMF). As shown in Fig. 4a and inset, the free probe displayed an emission peak with maximum at around 450 nm. By contrast, upon addition of H_2O_2 , the intensity of the emission peak at 450 nm gradually decreased with the simultaneous appearance of a new blue-shifted emission band centered at 560 nm. This result was similar with response of probe TPE-TLE to H_2O_2 in 50% PBS buffer solution (containing 50% DMF). Moreover, as shown in Fig. S4b, the probe TPE-TLE exhibited higher sensitivity (Detection limit: 1 μ M) in PBS buffer solution (containing 10% DMF) than 50% PBS buffer solution (containing 50% DMF). Furthermore, selectivity experiment indicated that the probe has high selectivity for H_2O_2 in 10% PBS buffer solution (containing 10% DMF) (Fig. S4c and d). The above results demonstrated that probe TPE-TLE could ratiometric detect H_2O_2 in 10% PBS buffer solution (containing 10% DMF).

We investigated influence of the probe TPE-TLE to H_2O_2 under different pH conditions. The results revealed that the pH value of solution had a notable influence on the probe response to H_2O_2 . As shown in Fig. S4, in the presence of H_2O_2 , the fluorescence intensity at 550 nm of probe response to H_2O_2 had no changes with the value increase of pH in the range of 5.0–8.0. In the absence of H_2O_2 , the free probe TPE-TLE exhibited weak fluorescence intensity in the wide pH range. The above results demonstrated that the TPE-TLE can respond well to H_2O_2 without dramatic influenced by pH.

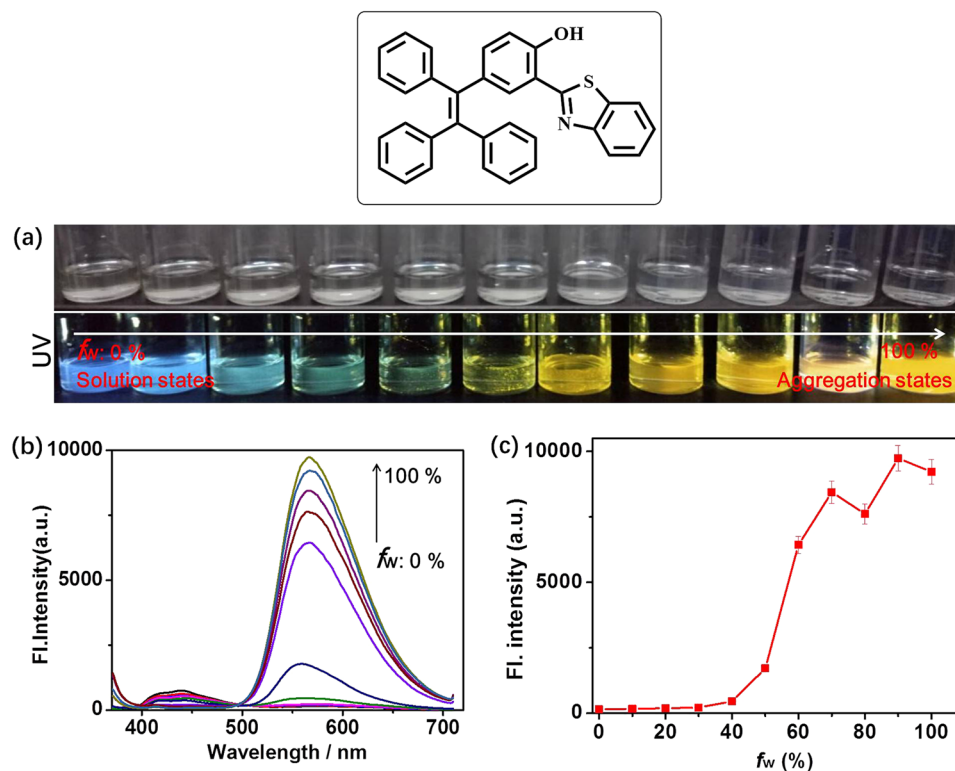


Figure 5. (a) Photographs of TPE-TLE-O in water/DMF mixtures taken under nature light and UV illumination; (b) Fluorescence spectra of TPE-TLE-O in water/DMF mixture; (c) Plots of maximum emission intensity of TPE-TLE-O in water/DMF mixtures with different f_w values. [TPE-TLE] = 5.0 μM . λ_{ex} = 365 nm. The error bars represent standard deviation (\pm S.D.).

Living cell imaging studies in RAW264.7 macrophages. In order to be useful as ratiometric imaging agents, ratiometric fluorescent probe should have low cytotoxicity. Thus, we investigated the potential toxicities of TPE-TLE against a representative cell: RAW264.7 macrophages. The living cells were incubated with various concentrations of the new ratiometric probe for 24 h, and then the cell viability was determined by the standard 3-(4,5-dimethylthiazol-2-yl)-2,5-diphenyltetrazolium bromide (MTT) assays; The results indicated that the ratiometric probe do not exhibit marked cytotoxicity (Fig. S5).

As we know, H_2O_2 widely exists in RAW 264.7 macrophages and plays key role in apoptosis and oxidative stress³³. Thus, to prove the capability of the probe TPE-TLE for H_2O_2 ratiometric fluorescence imaging in living cells, TPE-TLE (8 μM) was incubated with living RAW 264.7 macrophages for 0.5 h at 37 $^\circ\text{C}$, and then confocal imaging was carried out. As shown in Fig. 7, cells emitted a strong blue fluorescence signal and weak red fluorescence in the blue (Fig. 7b) and red channels (Fig. 7c), respectively. Because endogenous H_2O_2 will be produced by stimulating RAW264.7 macrophage cells using 12-myristate-13-acetate (PMA). Then TPE-TLE (8 μM) was incubated with living RAW 264.7 macrophages treated with PMA for 0.5 h at 37 $^\circ\text{C}$, and further achieved cells imaging. Imaging results demonstrated that cells displayed a slight blue emission (Fig. 7e) and a strong red emission (Fig. 7f), consistent with the H_2O_2 -induced ratiometric fluorescent response *in vitro*. Moreover, we further obtained ratiometric fluorescence imaging picture of both channels in living RAW 264.7 macrophages (Fig. 7g). The above results indicated that the probe TPE-TLE was capable of ratiometric imaging endogenous H_2O_2 in living RAW 264.7 macrophages by an aggregation emission method. The ratios of emission intensities profiles further prove that the TPE-TLE emitted stronger fluorescent intensity in living RAW 264.7 macrophages treated with PMA than RAW 264.7 macrophages untreated with PMA (Fig. 7h). This result was agreement with H_2O_2 -induced ratiometric fluorescent response *in vitro*.

Living cell imaging studies in cancer cells HepG2. It has been known for many years that H_2O_2 plays a major role in the progression of human illnesses, perhaps most importantly, cancer³⁴. To demonstrate the probe TPE-TLE ratiometric imaging exogenous H_2O_2 , the living cancer cells HepG2 and HepG2 treated with PMA were prepared. Imaging results indicated that cells untreated with PMA gave a strong blue fluorescence signal and a weak red signal in blue and red channels, respectively (Fig. 8a–c). However, images of cells treated with PMA results demonstrated that cells displayed a strong blue emission (Fig. 8e) and a strong red emission (Fig. 8f). Similarly with RAW 264.7 macrophages, ratiometric fluorescence imaging picture (Fig. 8g) and fluorescence emission profiles (Fig. 8h) were obtained. Thus, the above results establish that TPE-TLE is cell-membrane permeable ratiometric probe with AIE property, and suitable for the ratiometric imaging exogenous H_2O_2 in the living HepG2 cells by an aggregation emission method.

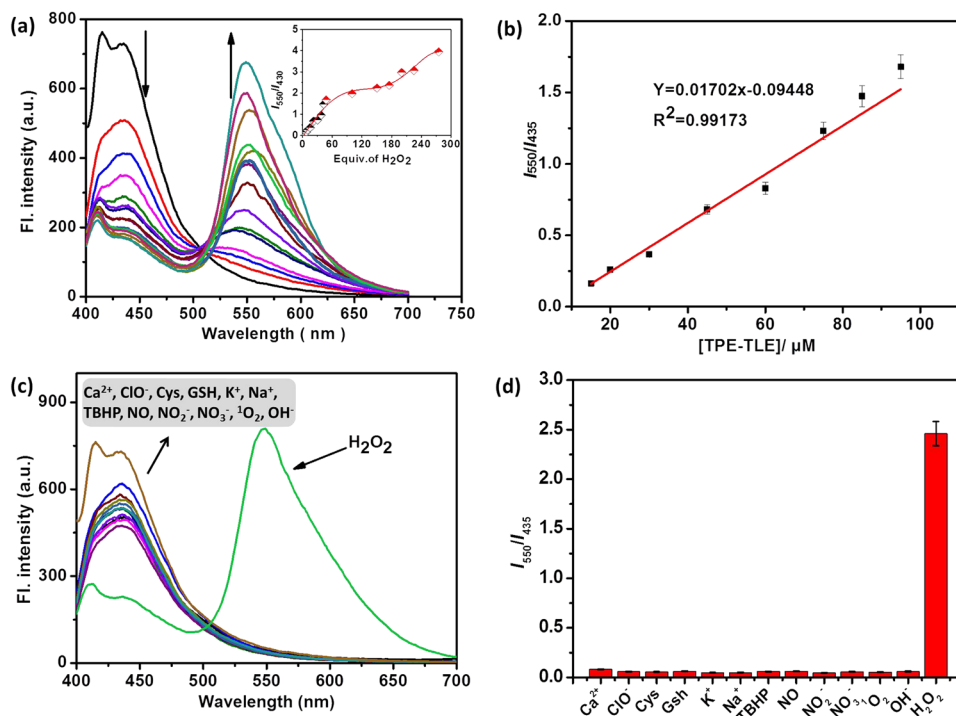


Figure 6. (a) Fluorescence spectra of TPE-TLE (5.0 μM) in pH 7.4 PBS buffer solution (containing 50% DMF) with the addition of H_2O_2 (0–200 equiv.). Inset: the fluorescence intensity changes at I_{550}/I_{435} of TPE-TLE with the amount of H_2O_2 . (b) Normalized response of the fluorescence signal by changing the concentration of H_2O_2 . $\lambda_{\text{ex}} = 380 \text{ nm}$. (c) Fluorescence spectra of TPE-TLE (5 μM) in the presence of various relevant analytes. (d) Fluorescence responses of TPE-TLE (5 μM) at 550 nm in the presence of various relevant analytes. The concentrations of the representative analytes are: amino acids, 1 mM; GSH, 2 mM; cations and anions, 3 mM; reactive oxygen and nitrogen species, 0.2 mM. The error bars represent standard deviation (\pm S.D.).

Compared to RAW 264.7 macrophages, both channels exhibited stronger fluorescence in living HepG2 cells than RAW 264.7 macrophages in the absence and presence of PMA. Moreover, the TPE-TLE probe emitted stronger red fluorescence in HepG2 cells treated with PMA than RAW 264.7 macrophages. Furthermore, the TPE-TLE exhibited higher ratio of emission intensities in HepG2 cells treated with PMA than RAW 264.7 macrophages. The above results demonstrated that cancer cells should contain more H_2O_2 than macrophages.

To the best of our knowledge, no reports to date have been published on the construction of ratiometric H_2O_2 fluorescent probes with AIE property for ratiometric fluorescent imaging endogenously H_2O_2 in RAW 264.7 macrophage and HepG2 cells.

Conclusions

In summary, we introduced a thiazole group and a borate moiety on the TPE-core to afford a novel ratiometric H_2O_2 probe TPE-TLE with AIE property for the first time. For sensing mechanism of TPE-TLE, in the presence of H_2O_2 , the oxidation reaction of H_2O_2 to the borate moiety will provide TPE-TLE-O, which will decrease aggregation fluorescence signal of TPE-TLE to induce aggregation fluorescence signal of TPE-TLE-O. Furthermore, the TPE-TLE exhibits excellent properties including the well-resolved emission peaks, high sensitivity, high selectivity, low cytotoxicity, and good cell-membrane permeability. The above mechanism and attributes enable us to demonstrate, for the first time, the ratiometric imaging of endogenously produced H_2O_2 in macrophages and cancer cells. Moreover, by comparing to fluorescence and ratio of emission intensities of both cells, it is firstly found that cancer cells should contain much more endogenous H_2O_2 than macrophages. We expect that TPE-TLE will be useful fluorescent platform for the development of a variety of ratiometric fluorescent probes with AIE property, and further achieve unique biological applications.

Methods

General procedure for the spectral measurement. The stock solution of the probe TPE-TLE was prepared at 1 mM in DMSO. The PBS (pH = 7.4) solutions with 50% DMSO was prepared. The solutions of various testing species were prepared from NaCl, KCl, CaCl₂, glutathione (GSH), H_2O_2 , homocysteine (Hcy), cysteine (Cys), NaNO₂, NaOH, t-butylhydroperoxide, NaClO, in the twice-distilled water. The test solution of the probe TPE-TLE (5 μM) were 50% PBS buffer solution (containing 50% DMF) and 90% PBS buffer solution (containing 10% DMF). The resulting solution was shaken before measuring the spectra. For titration and selectivity experiments of probe, both experiments were carried out using excitation wavelength of 405 nm, and the excitation and emission slit widths of the spectral measurement were 5 and 5 nm, respectively.

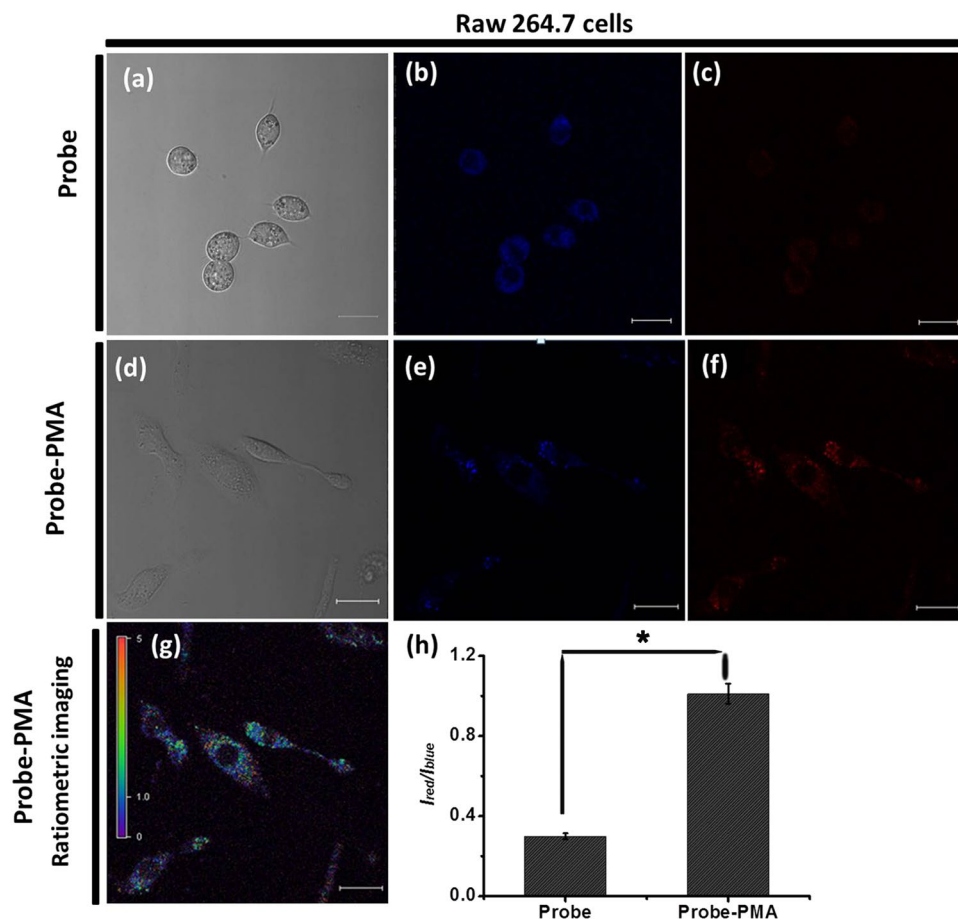


Figure 7. Image of endogenous H_2O_2 in RAW 264.7 cells untreated and treated with PMA. (a) Bright-field image of cells untreated with PMA, (b) Images of cells untreated with PMA in the blue emission channel ($\lambda_{ex} = 405$ nm, $\lambda_{em} = 425$ – 475 nm); (c) Images of cells untreated with PMA in the red emission channel ($\lambda_{ex} = 405$ nm, $\lambda_{em} = 570$ – 620 nm); (d) Bright-field images of cells treated with PMA; (e) Images of cells treated with PMA in the blue emission channel ($\lambda_{ex} = 405$ nm, $\lambda_{em} = 425$ – 475 nm); (f) Images of cells treated with PMA in the red emission channel ($\lambda_{ex} = 405$ nm, $\lambda_{em} = 570$ – 620 nm); (g) Ratiometric image of cells untreated with PMA; (h) The ratio of emission intensities profiles in RAW 264.7 cells untreated and treated with PMA. Scale bar = 20 μ m. Statistical analyses were performed with a Student's *t*-test ($n = 4$). * $P < 0.001$ and the error bars represent standard deviation (\pm S.D.).

Quantum yields. The fluorescence quantum yields would be calculated by the following formula (1):

$$\Phi_s = \Phi_r \left(\frac{A_r}{A_s} \right) \left(\frac{n_s^2}{n_r^2} \right) \frac{I_s}{I_r} \quad (1)$$

In this formula, *s* and *r* stand for the sample and the reference, respectively. Φ stands for quantum yield; *F* and *A* stands for the integrated emission intensity and the absorbance, respectively; *n* is refractive index³⁵.

Cytotoxicity assay. Living RAW264.7 cells were cultivated in per well of 96-well plate. After 24 h, the culture medium was changed using new culture medium containing different concentration (0 μ M, 1 μ M, 5 μ M, 10 μ M, 20 μ M) TPE-TLE. After 8 h, the culture medium and the excess probes were removed, and then 10 μ L MTT (5 mg/mL in PBS) was added to the above medium. Subsequently, the culture medium was removed, and 100 μ L DMSO was added to the 96-well plate in order to dissolve the formazan crystal product. The plate containing Living RAW264.7 cells was shaken for 10 min, and then the plate containing RAW264.7 cells was measured at 490 nm using the microplate reader. OD₄₉₀ sample denotes the RAW264.7 cells incubated with the probe TPE-TLE at different incubation times, OD₄₉₀ control denotes the RAW264.7 cells without the probe TPE-TLE, OD₄₉₀ blank denotes the wells containing only the culture medium. The cell viability would be calculated by the following formula: Cells viability (%) = (OD₄₉₀ sample – OD₄₉₀ blank)/(OD₄₉₀ control – OD₄₉₀ blank) \times 100%^{36,37}.

Cells culture. Living RAW264.7 macrophages were prepared in H-DMEM (Dulbecco's Modified Eagle's Medium, High Glucose) supplemented with 10% fetal bovine serum in a 5% CO₂ incubator at 37 $^{\circ}$ C. Before the living cells imaging experiments, living RAW264.7 cells were seeded confocal dish (density of cells was 1×10^5 /

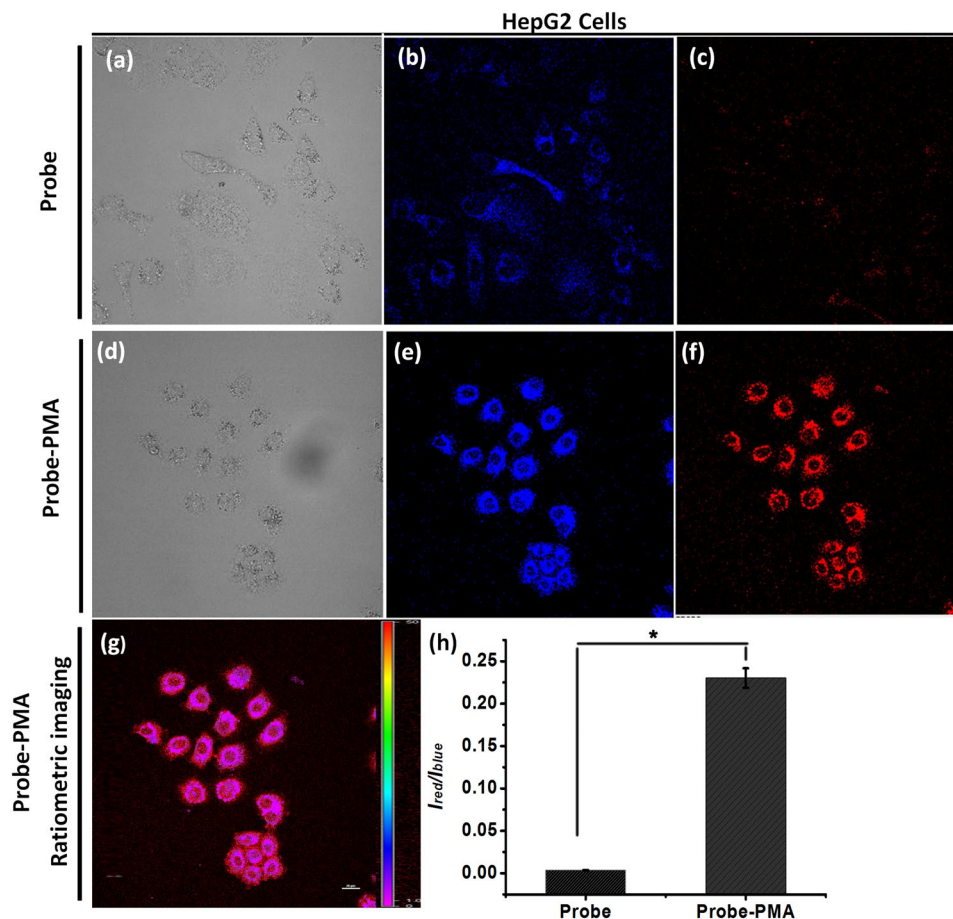


Figure 8. (a) Bright-field image of cells untreated with PMA, (b) Images of cells untreated with PMA in the blue emission channel ($\lambda_{\text{ex}} = 405 \text{ nm}$, $\lambda_{\text{em}} = 425\text{--}475 \text{ nm}$); (c) Images of cells untreated with PMA in the red emission channel ($\lambda_{\text{ex}} = 405 \text{ nm}$, $\lambda_{\text{em}} = 570\text{--}620 \text{ nm}$); (d) Bright-field images of cells treated with PMA; (e) Images of cells treated with PMA in the blue emission channel ($\lambda_{\text{ex}} = 405 \text{ nm}$, $\lambda_{\text{em}} = 425\text{--}475 \text{ nm}$); (f) Images of cells treated with PMA in the red emission channel ($\lambda_{\text{ex}} = 405 \text{ nm}$, $\lambda_{\text{em}} = 570\text{--}620 \text{ nm}$); (g) Ratiometric images of cells untreated with PMA. (h) The ratio of emission intensities profiles in HepG2 cells untreated and treated with PMA. Scale bar = 20 μm . Statistical analyses were performed with a Student's *t*-test ($n = 4$). * $P < 0.001$ and the error bars represent standard deviation (\pm S.D.).

mL). The cells were placed on glass coverslips and allowed to adhere for 48 h. Cells imaging experiments could be carried out as soon as the cells reached about 70% confluence.

Firstly, control experiment was further carried out. The culture medium of the cells was added to a fresh medium containing 50.0 $\mu\text{g/mL}$ 12-myristate-13-acetate (PMA) and incubated for 3 h. Secondly, the medium was removed and washed three times with PBS in order to remove the excess PMA. After that, 1 mL of the medium containing 8 μM TPE-TLE was added and further incubated at 37 $^{\circ}\text{C}$ for 30 min. Finally, the confocal imaging was carried out in the blue ($\lambda_{\text{ex}} = 405 \text{ nm}$, $\lambda_{\text{em}} = 425\text{--}475 \text{ nm}$) and green channels ($\lambda_{\text{ex}} = 405 \text{ nm}$, $\lambda_{\text{em}} = 570\text{--}620 \text{ nm}$) using Nikon AMP1 confocal microscopy.

Synthesis of 1. The compound was synthesized by refer literature³⁸.

Synthesis of TPE-TLE-O. In a round-bottomed flask (25 mL) equipped with a magnetic stirrer, a solution of the compound 1 (0.37, 1.0 mmol) and 2-aminothiophenol (0.15 g, 1.2 mmol) in methanol (10 mL) was prepared. Then, 30% H_2O_2 (6.0 mmol) and 37% HCl (3.0 mmol) were added and the mixture was stirred at room temperature for 2 h. The mixture was quenched by adding H_2O (10 mL), extracted with EtOAc (3 5 mL), and the combined extracts were dried (Na_2SO_4). The corresponding benzothiazoles were obtained after removal of solvents and purified by silica gel chromatography (eluent: n-hexane/EtOAc = 4:1). The yield of TPE-TLE-O was 65%. ^1H NMR (400 MHz, CDCl_3) δ 12.47 (s, 1H), 7.99–7.94 (m, 1H), 7.85 (dd, $J = 8.0, 1.1 \text{ Hz}$, 1H), 7.50 (m, 1H), 7.42–7.35 (m, 2H), 7.20–7.02 (m, 16H), 6.88 (d, $J = 8.6 \text{ Hz}$, 1H). ^{13}C NMR (101 MHz, $\text{DMSO-}d_6$) δ 155.39, 151.77, 143.78, 143.45, 140.09, 135.41, 135.07, 131.26, 131.12, 128.44, 128.38, 128.29, 127.16, 127.03, 126.94, 125.52, 122.54, 122.41, 116.95.

Synthesis of TPE-TLE. Compound 2 (0.24 g, 0.5 mmol) was added into a flask containing a mixture of 4-bromomethylphenyl boronic acid (0.15 g, 0.5 mmol), K_2CO_3 (0.07 g, 0.5 mmol), and 10 mL of DMF with nitrogen at room temperature for 6 h, then poured into H_2O (500 mL) and extracted with EtOAc. The organic phase was separated, dried with $MgSO_4$, and removed by vacuum distillation. The product was obtained as a yellow solid with a yield of 60% after purified by column chromatography with ethyl acetate/petroleum ether (2:1, v/v) as eluent. Melting point: 142–146 °C. 1H NMR (400 MHz, DMSO-*d*₆) δ 8.10 (s, 1H), 8.05–8.07 (d, *J* = 8.0 Hz, 1H), 7.95–7.97 (d, *J* = 8.4 Hz, 1H), 7.71–7.73 (d, *J* = 7.6 Hz, 2H), 7.56–7.58 (d, *J* = 8.0 Hz, 2H), 7.48–7.57 (t, *J* = 7.8 Hz, 1H), 7.38–7.46 (t, *J* = 7.4 Hz, 1H), 6.99–7.16 (m, 17H), 5.40 (s, 2H), 1.30 (s, 12H). ^{13}C NMR (101 MHz, DMSO) δ 162.21, 154.88, 151.80, 143.63, 143.55, 143.37, 141.36, 139.89, 139.80, 136.73, 135.77, 135.15, 135.08, 131.30, 131.21, 131.11, 128.42, 128.30, 127.96, 127.19, 127.03, 126.71, 125.38, 122.86, 122.25, 121.51, 113.71, 84.19, 70.82, 40.65, 40.44, 40.24, 40.03, 39.82, 39.61, 39.40, 25.16. HRMS (ESI) (*m/z*): [*M* + *H*]⁺ calcd for $C_{46}H_{40}BNO_3S$: 698.3000, found, 698.3001.

References

- Luo, J. *et al.* Aggregation-induced emission of 1-methyl-1,2,3,4,5-pentaphenylsilole. *Chem. Commun.* **18**, 1740–1741 (2001).
- Hong, Y., Lam, J. W. Y. & Tang, B. Z. Aggregation-induced emission. *Chem. Soc. Rev.* **40**, 5361–5388 (2011).
- Sagara, Y., Yamane, S., Mitani, M., Weder, C. & Kato, T. Mechanoresponsive luminescent molecular assemblies: An emerging class of materials. *Adv. Mater.* **28**, 1073–1076 (2016).
- Hu, R., Leung, N. L. C. & Tang, B. Z. AIE macromolecules: syntheses, structures and functionalities. *Chem. Soc. Rev.* **43**, 4494–4562 (2014).
- Li, K. & Liu, B. Polymer-encapsulated organic nanoparticles for fluorescence and photoacoustic imaging. *Chem. Soc. Rev.* **43**, 6570–6597 (2014).
- Ding, D., Li, K., Liu, B. & Tang, B. Z. Bioprobes based on AIE fluorogens. *Acc. Chem. Res.* **46**, 2441–2453 (2013).
- Kemp, M. L. 2013, Reactive Oxygen Species (ROS) [M]. *Springer New York* (2013).
- Ray, P. D., Huang, B. W. & Tsuji, Y. Reactive oxygen species (ROS) homeostasis and redox regulation in cellular signaling. *Cellular Signalling* **24**, 981–990 (2012).
- Thannickal, V. J. & Fanburg, B. L. Reactive oxygen species in cell signaling. *Am. J. Physiol. Lung Cell. Mol. Physiol.* **279**, L1005–L1028 (2000).
- Mata, M., Pallardo, F., Morcillo, E. J. & Cortijo, J. Piclamilast inhibits the pro-apoptotic and anti-proliferative responses of A549 cells exposed to H_2O_2 via mechanisms involving AP-1 activation. *Free Radical Research* **46**, 690–699 (2012).
- Agbor, G. A. *et al.* Antioxidant capacity of some plants foods and beverages consumed in the eastern region of Nigeria. *AJTCAM* **8**, 362–369 (2011).
- Marcocci, C., Leo, M. & Altea, M. A. Oxidative stress in Graves' disease. *Eur. Thyroid. J.* **1**, 80–87 (2012).
- Brenneisen, P., Briviba, K., Wlaschek, M., Wenk, J. & Scharffetter-Kochanek, K. Hydrogen peroxide (H_2O_2) increases the steady-state mRNA levels of collagenase/MMP-1 in human dermal fibroblasts. *Free Radic. Biol. Med.* **22**, 515–524 (1977).
- Courgeon, A. M., Rollet, E., Becker, J., Maisonhaute, C. & Best-Belpomme, M. *Eur. J. Biochem.* **171**, 163–170 (1988).
- Näther, N. *et al.* *Sensors* **6**, 308–317 (2006).
- James, O. & Alewo, I. M. *In vitro* antihemolytic activity of gymnema sylvestre extracts against hydrogen peroxide (H_2O_2) induced haemolysis in human erythrocytes. *AJPCT* **2**, 861–869 (2014).
- Brankiewicz, W. & Trebacz, K. The impact of hydrogen peroxide (H_2O_2) to the bioelectric signals in the liverwort *Conocephalum conicum*. *Acta Medica Academiae Scientiarum Hungaricae* **5**, 169–174 (2014).
- Karisch, R. & Neel, B. G. Methods to monitor classical protein-tyrosine phosphatase oxidation. *FEBS. J.* **280**, 459–475 (2013).
- Lennicke, C., Rahn, J., Lichtenfels, R., Wessjohann, L. A. & Seliger, B. Hydrogen peroxide – production, fate and role in redox signaling of tumor cells. *Cell. Commun. Signal.* **13**, 39–57 (2015).
- Behl, C., Davis, J. B., Lesley, R. & Schubert, D. *Cell* **77**, 817–827 (1994).
- Imlay, J. A., Chin, S. M. & Linn, S. *Science* **240**, 640–642 (1988).
- Lópezlázaró, M. Dual role of hydrogen peroxide in cancer: possible relevance to cancer chemoprevention and therapy. *Cancer Lett.* **252**, 1–8 (2007).
- Lisanti, M. P. *et al.* Hydrogen peroxide fuels aging, inflammation, cancer metabolism and metastasis: The seed and soil also needs “fertilizer”. *Cell Cycle* **10**, 2440–2449 (2011).
- Fujikawa, Y., Morgan, B. & Dick, T. P. Fluorescent Imaging of Redox Species in Multicellular Organisms. *Springer Netherlands*. 119–155 (2013).
- Lippert, A. R., Bittner, G. C. V. D. & Chang, C. J. *Accounts. Chem. Res.* **44**, 793–804 (2011).
- Dong, B. *et al.* *Adv. Mater.* **28**, 8755–8758 (2016).
- Zhao, Z.-J. *et al.* Using tetraphenylethene and carbazole to create efficient luminophores with aggregation-induced emission, high thermal stability, and good hole-transporting property. *J. Mater. Chem.* **22**, 4527–4534 (2012).
- Liu, Y., Meng, F., He, L., Yu, X. & Lin, W. Fluorescence behavior of a unique two-photon fluorescent probe in aggregate and solution states and highly sensitive detection of RNA in water solution and living systems. *Chem. Commun.* **52**, 8838–8841 (2016).
- Goodall, W. & Williams, J. A. A new, highly fluorescent terpyridine which responds to zinc ions with a large red-shift in emission. *Chem. Commun.* **23**, 2514–2515 (2001).
- He, L., Dong, B., Liu, Y. & Lin, W. Fluorescent chemosensors manipulated by dual/triple interplaying sensing mechanisms. *Chem. Soc. Rev.* **45**, 6449–6461 (2016).
- Howells, R. D. *et al.* Localization of striatal opioid gene expression, and its modulation by the mesostriatal dopamine pathway: An *in situ* hybridization study. *Proc. Natl. Acad. Sci. USA* **81**, 7651–7655 (1984).
- Jacob, J. *et al.* Biogeochemical characteristics of the surface sediments along the western continental shelf of India. *Chem. Ecol.* **25**, 135–139 (2009).
- Karabay, Z. A., Özkan, T., Koç, A. & Büyükbıngöl, Z. Effects of MSM (methylsulfonylmethane) on SNP (sodium nitroprusside) and H_2O_2 (hydrogen peroxide) induced RAW 264.7 macrophages. *Planta Med.* **75**, 911–911 (2009).
- Park, I. J. *et al.* Green tea catechin controls apoptosis in colon cancer cells by attenuation of H_2O_2 -stimulated COX-2 expression via the AMPK signaling pathway at low-dose H_2O_2 . *Ann. N.Y. Acad. Sci.* **1171**, 538–544 (2009).
- Ding, S., Zhang, Q., Xue, S. & Feng, G. Real-time detection of hypochlorite in tap water and biological samples by a colorimetric, ratiometric and near-infrared fluorescent turn-on probe. *Analyst* **13**, 4687–4693 (2015).
- Ding, S. & Feng, G. Smart probe for rapid and simultaneous detection and discrimination of hydrogen sulfide, cysteine/homocysteine, and glutathione. *Sens. Actuators B* **235**, 691–697 (2016).
- Huang, Z., Ding, S., Yu, D., Huang, F. & Feng, G. Aldehyde group assisted thiolysis of dinitrophenyl ether: a new promising approach for efficient hydrogen sulfide probes. *Chem. Commun.* **50**, 9185–9187 (2014).
- Feng, H. T., Song, S., Chen, Y. C. & Zheng, Y. -S. Self-assembled tetraphenylethylene macrocycle nanofibrous materials for the visual detection of copper (II) in water. *J. Mater. Chem. C* **2**, 2353–2359 (2014).

Acknowledgements

This work was financially supported by NSFC (51503077, 21472067, 21672083), Taishan Scholar Foundation (TS 201511041), and the startup fund of the University of Jinan (309-10004). Doctor start up fund of University of Jinnan (160082102) and NSFSP (ZR2015PE001).

Author Contributions

W. Lin and Y. Liu conceived the idea and directed the work. Y. Liu and J. Nie designed the experiments and performed the organic synthesis and spectral measurements. Y. Liu, J. Niu and F. Meng performed the bioimaging. All authors contributed to data analysis, manuscript writing and participated in research discussions.

Additional Information

Supplementary information accompanies this paper at doi:[10.1038/s41598-017-07465-5](https://doi.org/10.1038/s41598-017-07465-5)

Competing Interests: The authors declare that they have no competing interests.

Publisher's note: Springer Nature remains neutral with regard to jurisdictional claims in published maps and institutional affiliations.



Open Access This article is licensed under a Creative Commons Attribution 4.0 International License, which permits use, sharing, adaptation, distribution and reproduction in any medium or format, as long as you give appropriate credit to the original author(s) and the source, provide a link to the Creative Commons license, and indicate if changes were made. The images or other third party material in this article are included in the article's Creative Commons license, unless indicated otherwise in a credit line to the material. If material is not included in the article's Creative Commons license and your intended use is not permitted by statutory regulation or exceeds the permitted use, you will need to obtain permission directly from the copyright holder. To view a copy of this license, visit <http://creativecommons.org/licenses/by/4.0/>.

© The Author(s) 2017